Engineering Structures 267 (2022) 114629

Contents lists available at ScienceDirect

Engineering Structures

journal homepage: www.elsevier.com/locate/engstruct

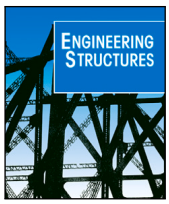

Dynamic response of driven end-bearing piles and a pile group in soft clay: an experimental validation study

Freddie Theland [a,*], Geert Lombaert [b], Stijn François [b], Costin Pacoste [a,c], Fanny Deckner [d], Peter Blom [e], Jean-Marc Battini [a]

[a] KTH Royal Institute of Technology, Division of Structural Engineering and Bridges, Brinellvägen 23, 100 44 Stockholm, Sweden
[b] KU Leuven, Department of Civil Engineering, Kasteelpark Arenberg 40, 3001 Leuven, Belgium
[c] ELU Konsult AB, Valhallavägen 117, 115 31 Stockholm, Sweden
[d] GeoMind KB, Hesselmans Torg 5, 131 54 Nacka, Sweden
[e] ACAD International AB, Sveavägen 151, 113 46 Stockholm, Sweden

ARTICLE INFO

Keywords:
End-bearing piles
Dynamic impedance
Soil–structure interaction
Pile group
Environmental vibration
Pile–soil–pile interaction

ABSTRACT

This paper presents novel measurement data on the dynamic soil–structure interaction of an end-bearing pile foundation. The purpose is to assess the ability to predict the foundation impedances based on the small-strain properties of the soil obtained from site investigations. Measurements were performed in two stages of construction, allowing to assess interaction between the piles through the soil. First, single pile impedances and interaction factors between the piles were experimentally obtained for the four piles when they were free to move at the surface. Second, the impedances of the square pile group were measured after casting a concrete pile cap. The piles were additionally instrumented with accelerometers at depth along the centerline of each pile, allowing to illustrate the global behaviour of the piles within the soil. Numerical predictions based solely on information of the small-strain soil properties obtained from extensive site investigations are compared to the experimental results. The impedances of the individual piles are overestimated compared to the measurements, while the interaction factors show a better agreement. The pile group impedances are better captured than the individual ones, using the same soil model. The pile–soil–pile interaction is clearly manifested in the experimental results by pronounced peaks in the pile group vertical impedance, validating results from previous numerical studies.

1. Introduction

Dynamic soil–structure interaction can have an important influence on the dynamic structural response for applications in earthquake engineering, railway bridge dynamics, machine foundation design and environmental vibration assessment. In Sweden, the geological conditions generally consist of clay, silt or sand overlaying a densely compacted moraine (till) and crystalline bedrock. Formations of cohesive soils are often found in the more densely populated regions and major cities. These site conditions motivate the use of driven end-bearing piles for foundation design, where prefabricated concrete piles are predominantly used [1,2].

Under the assumption of small deformations in the soil, soil–structure interaction can be modelled using a linear elastic model, which allows for separation of the soil-foundation system from the overlying structure in a substructuring scheme [3]. The interaction between the foundation and the soil can be condensed into dynamic impedance functions, characterising the effective stiffness and damping of the soil-foundation system that can subsequently be coupled to an overlying structure. The computation of the dynamic impedance functions of pile foundations from analytical and numerical models have been extensively treated in the literature, showing the significant influence of the interaction between piles through the soil. However, there is lack of experimental evidence of the validity of models of end-bearing piles and pile groups in shallow formations of soils over bedrock, where the distribution of pile displacements differ from the case of floating piles and layer resonances can influence the dynamic response. Existing modelling strategies to obtain the impedances of pile foundations include simplified models providing approximate pile group impedances by superposition of pile–soil–pile interaction factors [4–8], hidden

* Corresponding author.
E-mail addresses: freddie.theland@byv.kth.se (F. Theland), geert.lombaert@kuleven.be (G. Lombaert), stijn.francois@kuleven.be (S. François), costin.pacoste@elu.se (C. Pacoste), fanny.deckner@geomind.se (F. Deckner), peter.blom@acad.se (P. Blom), jean-marc.battini@byv.kth.se (J.-M. Battini).

https://doi.org/10.1016/j.engstruct.2022.114629
Received 10 December 2021; Received in revised form 9 May 2022; Accepted 30 June 2022
Available online 26 July 2022

state variable models [9], Beam-on-dynamic Winkler foundation approaches [10,11] as well as more rigorous solutions using boundary integral, boundary- and finite element model formulations [12–14]. Models have facilitated the analysis of the dynamic behaviour of piles and pile groups, and led to a deeper understanding of the factors influencing the dynamic impedances of piles and pile groups. Gazetas and Makris [15] demonstrated that the main features of pile–soil–pile interaction that influence the vertical and horizontal [16] impedances of pile groups are governed by the pile-to-pile spacing and the small-strain properties of the soil, resulting in a dramatic increase in group stiffness and damping values at certain frequencies. It was also shown that the variation of soil properties with depth can substantially influence the predicted group impedances as it influences the wave field generated by the excited piles. Therefore, an accurate representation of the soil is crucial for the prediction of the dynamic foundation impedances. Padrón et al. [13] used a coupled finite element-boundary element model to present a set of dynamic impedance functions for end-bearing pile groups and a comparison to their floating counterpart for square foundations with 2×2 and 3×3 vertical and battered piles in homogeneous soil deposits. The presence of bedrock was shown to influence the dynamic vertical and rotational impedances of the pile groups substantially, especially for soft soils, while the horizontal impedance was only significantly affected for configurations where piles were inclined.

To confide in the results derived from models, validation by experiments is necessary. A number of experimental studies have been performed under field conditions to validate numerical predictions of the response of floating single piles [17–21] and pile groups in cohesive [22–27] and non-cohesive soils [28–32]. The majority of the experimental studies in the literature have been focused on the excitation and response in the lateral direction and only a handful of experimental results have been presented for the vertical response of pile groups. Novak and Grigg [33] performed experiments on single piles and 2×2 pile groups driven in a soil consisting of silty sand and till to analyse the response due to both vertical and lateral excitations. Variation of the soil's shear modulus with depth and the floating condition at the pile tip were found to be important factors to take into account when comparing the measurements to results obtained from a numerical model. Manna and Baidya [34] performed an experimental study on the non-linear vertical response of cast in situ piles and a 2×2 pile group and compared the results to numerical simulations using an equivalent linear approach with a weakened boundary zone closest to the piles, finding a reasonable agreement. Capatti et al. [35] performed extensive dynamic testing to characterise the translational and rotational response of a 2×2 pile foundation with inclined steel micropiles in an alluvial silt subjected to different amplitudes of dynamic loading. The piles were instrumented with strain gauges and the natural frequencies of the system and the deformation of the piles were found to be influenced by gapping of the most superficial soil, induced by the high amplitude dynamic loads. In a series of small-scale laboratory experiments in a sand [36–39], lateral pile–soil–pile interaction and pile group impedance were studied, considering the influence of non-linear loading conditions. Interaction factors were established for different load amplitudes and compared to linear theory. Dezi et al. [40] measured the response of three large-diameter steel pipe piles installed at a near-shore location in a marine clay when subjected to controlled impact loading, allowing to characterise the interaction between the piles through the soil under field conditions.

In the aforementioned experiments, interaction effects associated with a group stiffness larger than the sum of the stiffnesses of the individual piles are either expected to occur outside the considered frequency range or were not discussed. Therefore, there is a need to experimentally verify, in a full scale setting, the existence of these interaction phenomena predicted by theory. Moreover, while numerical results for end-bearing piles and pile groups have been presented in the literature [13,41], to the best of the authors' knowledge, no experimental studies have been published where a complete set of dynamic impedance functions is presented for an end-bearing pile foundation.

This paper presents the results from an extensive experimental measurement campaign of the dynamic response and impedances of a full scale concrete foundation supported by pre-cast impact driven end-bearing concrete piles installed in a soft clay deposit. The objectives of this paper are twofold. First, to present measurement data on the small-strain dynamic pile–soil–pile interaction and the impedances of end-bearing impact driven concrete piles and a pile group under typical Swedish soil conditions. The novelty of the experiments consists in the specific foundation and site conditions, where a full scale end-bearing pile foundation in soft clay is considered, and the extensive set of measurements performed during different stages of construction of the pile group, allowing to analyse the interaction between the piles and to verify its influence on the dynamic properties of the pile group experimentally. Second, to assess the ability of a linear elastic soil model to predict the dynamic characteristics of the soil-foundation system, using the small-strain soil properties obtained from site investigations. Here, it should be emphasised that a design condition has been considered. The numerical predictions are obtained from a model based solely on the performed soil investigations. No attempt to update this model to better match the experimental results has been performed. This corresponds to a class A prediction in accordance with the classification of predictions in geotechnical engineering proposed by Lambe [42].

The structure of the paper is as follows. Section 2 gives an overview of the test site and the identified small-strain properties at the site. Section 3 motivates and describes the design of the pile group. Section 4 presents a finite element model of the soil-foundation system. Section 5 presents the equipment, experimental setups and the post-processing of the measurements. Section 6 thereafter presents the dynamic responses and impedances of the free-top piles and the pile group and compares the measurements to numerical predictions. Section 7 concludes the paper.

2. Test site

2.1. Site overview

The test site is located 40 km north of Stockholm, Sweden. The site is a remotely located agricultural field that has not been cultivated for more than ten years prior to the experiments. It was chosen because of its particular stratification, with a soft clay underlain by till and bedrock, the possibility to represent the soil using a horizontally layered soil model and that unlimited access to the site could be granted. The soil conditions are representative for sites where impact driven piles are used. Moreover, as the site is located in a remote location, a minimum of environmental background vibration is present during testing. Fig. 1 presents an overview of the site and two sections of the soil interpreted from the site investigations, where the location of the pile group is indicated.

2.2. Soil conditions and small-strain properties

Extensive geotechnical and geophysical site investigations have been performed at the site. The geotechnical investigations consisted of weight soundings, soil-rock probing, cone penetration tests (CPT) and laboratory analysis of piston samples. The soil conditions at the site consist of 1 m dry crust clay followed by homogeneous gray, slightly varved clay with infusions of sand and silt up to 4.9 m depth where a sandy gravelly till overlays the bedrock to a depth of 7.4 m. The small-strain properties of the soil have been determined from in situ wave speed measurements by seismic cone penetration tests (SCPT) and spectral analysis of surface waves (SASW) performed at the location where the pile group is constructed. In addition, bender element tests have been performed on clay piston samples collected at the location

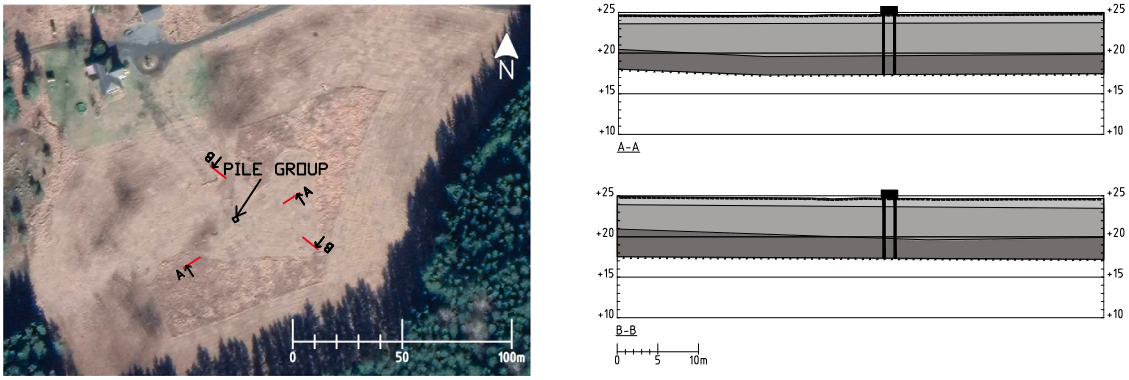

(a) (b)

Fig. 1. Overview of the site with (a) an aerial photography [43] with the location of the pile group indicated and (b) two sections with the stratification interpreted from geotechnical site investigations with a layering of dry crust clay (light gray), saturated soft clay (medium gray) and till (dark gray) on top of a stiff bedrock.

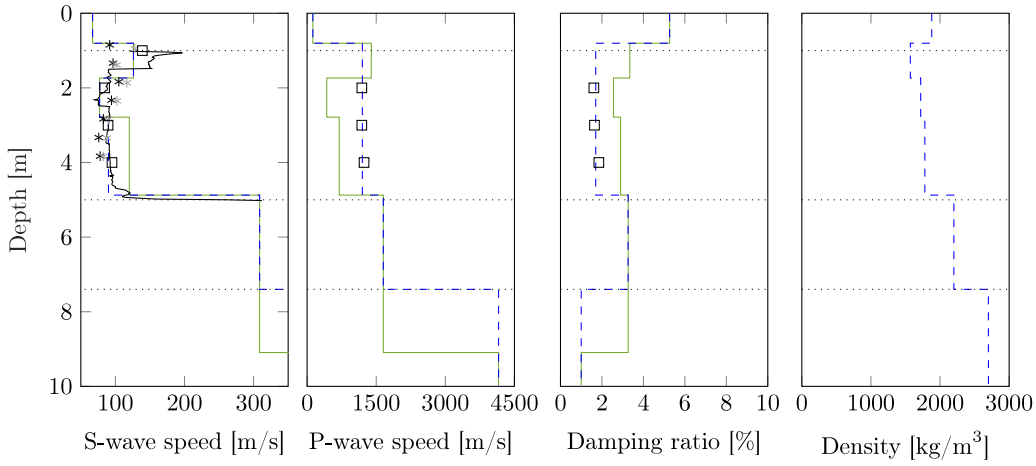

Fig. 2. Small-strain dynamic soil properties estimated from bender element tests (□), SCPT (*), empirical correlation with CPT (black line) and SASW (green line). A representative synthesised soil model (blue dashed line) taking into account the layer boundaries identified from soil/rock probing (dotted lines) is presented. (For interpretation of the references to color in this figure legend, the reader is referred to the web version of this article.)

where the pile group is constructed, to obtain estimates of material wave speeds and damping ratios. Empirical correlation with a CPT performed next to the point where the samples were collected has also been considered. Fig. 2 presents the estimated small-strain soil properties obtained from the different methods. A detailed description of the site investigations and evaluation of the estimated properties was given in Theland et al. [44]. The soil properties estimated using different methods are consistent in the upper three meters, but the deepest layer of clay is estimated to be stiffer by the SASW than by the other methods. Due to the larger body of soil covered by the SASW test, the spatial variability of the soil properties over the test area can affect the estimated soil profile, explaining the observed inconsistency. As the point wise investigations are in close agreement and were performed at the location where the piles were driven, the properties derived from these tests are considered as most reliable at this specific location. Table 1 presents the properties of the profile synthesised from the investigations that are used for modelling the soil.

Table 1
Estimated small-strain soil properties based on dynamic site and laboratory investigations.

Description	Layer	Depth [m]	h [m]	C_s [m/s]	C_p [m/s]	β_s [−]	β_p [−]	ρ [kg/m^3]
Dry crust clay	1	0.80	0.80	67	125	0.053	0.053	1880
Clay	2	1.73	0.93	126	1200	0.017	0.017	1570
Clay	3	2.78	1.05	77	1200	0.017	0.017	1720
Clay	4	4.87	2.09	90	1200	0.017	0.017	1780
Till	5	7.4	2.53	309	1654	0.033	0.033	2200
Bedrock	6	∞	∞	2236	4156	0.010	0.010	2700

3. Pile group design and installation

The pile group was designed to characterise a part of a foundation system for a multi-storey building carrying loads from e.g. a column. Therefore, vertical piles were used. The piles are pre-fabricated and made out of reinforced C50/60 concrete with a square 235 × 235 mm cross-section and equipped with steel toes, transferring the vertical loads to the bedrock in compression. The piles are assumed to have a density of $\rho_p = 2400$ kg/m^3 and a Poisson's ratio $\nu_p = 0.2$. The modulus of elasticity $E_p = 39$ MPa was tuned based on the natural frequencies obtained from an experimental modal analysis carried out in the factory, where one of the piles was suspended in springs to simulate free-free boundary conditions. The identified modulus agrees with the tangent modulus specified by the manufacturer.

To allow for installation of sensors within the piles after driving them at site, a cylindrical cavity was introduced along the center of the piles. This was achieved by installing a 76 mm diameter plastic pipe along the center line when casting the piles. The spacing between the piles was chosen to be representative for design solutions while at the same time highlighting the dynamic interaction between the piles,

especially in the vertical and rotational modes of vibration that are most affected by the end-bearing condition [13]. The pile–soil–pile interaction depends on the wavelengths of body waves in the soil relative to the separation distance between the piles [24,45]. In the literature, normalization of the frequency and the pile separation is commonly performed with reference to a pile diameter. The equivalent separation to pile diameter ratio of the pile group with square section piles is $s/d_{eq} = 5.15$, with the equivalent diameter defined as $d_{eq} = 2b/\sqrt{\pi}$ where b is the cross-section side length and the separation distance $s = 1.365$ m. For the soil conditions at the site, this situates the effects of pile–soil–pile interaction within the frequency band 1–80 Hz, covering the band of interest for environmental building vibrations [46].

The piles were installed at the site in February 2020 with a BANUT 550/Volvo EC280 impact pile driver with a fall-weight of 5 ton and a fall-height of 20–30 cm. The piles were driven to a stop, with a stopping criteria of 10 mm/10 impacts and were estimated to have reached bedrock. An apparent inclination of the bedrock surface was observed in the north-west direction as the piles came to a stop at different depths, resulting in the piles reaching a depth of 6.3 m for piles P2 and P3 positioned to the south-east and 5.6 m for P1 and P4 positioned to the north-west. This is either due to the natural variation of the bedrock surface, or an indication of the presence of a boulder where the piles were installed.

After performing measurements on the free-top piles, the pile group was joined in a reinforced $2 \times 2 \times 0.85$ m concrete pile cap. The cap is assumed to have the same material properties as the piles. Contact at the interface between the pile cap and the soil can influence the dynamic response of the pile group [33,34,47]. The contact condition between the cap and the soil can be difficult to model and in the case of end-bearing piles in soft soil the cap can separate from the soil when settlement takes place. Therefore, the pile cap was elevated 120 mm from the soil's surface to eliminate any interaction between the pile cap and the soil.

4. Numerical model

Numerical simulations are performed using the finite element method. The foundation and the soil are assumed to be linear elastic and the problem can therefore be solved in the frequency domain. The material properties of the soil are obtained from Table 1 and material damping is introduced as hysteretic damping by modifying the modulus of elasticity $E^* = E(1 + i2\beta)$, with $i^2 = -1$ defining the imaginary unit and where the damping ratios in deviatoric (β_s) and volumetric (β_p) deformation are implicitly assumed to be equal. Fig. 3 presents the model geometry considered for the simulations. The soil layers, piles and pile cap are modelled as a three dimensional solid body. The pipes in the piles are considered as cylindrical cavities introduced along the center line of the piles. Perfectly matched layers (PML) are adopted in the region closest to the outer boundary of the soil in order to attenuate any outgoing waves, representing the extension to infinity. The thickness of the PML domains is 2 m and the stretch functions proposed by Basu and Chopra [48] are applied to effectively attenuate both evanescent and propagating waves. The attenuation profile in the PML region is linear with scaling factors for evanescent and propagating waves both equal to 10. The PML region is discretized by quadratic hexahedra solid elements while quadratic tetrahedra elements are used for the piles, the concrete cap and the soil within the computational domain. The maximum prescribed element size is determined such that a minimum resolution of five quadratic elements per wavelength in the soil are present in the considered frequency range, resulting in a minimum element size of 0.17 m in the top soil layer. The mesh is verified to yield converged results in the frequency range of interest. In the case where the pile group is joined at the surface by the concrete cap, the symmetry of the problem is exploited to reduce the computational effort.

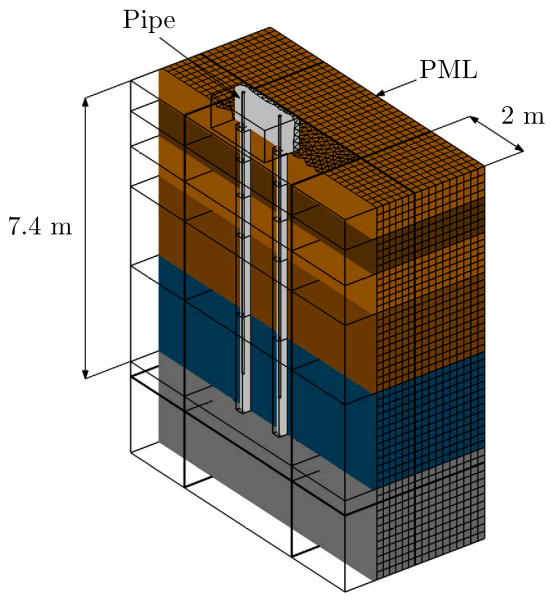

Fig. 3. Section of the finite element model of the pile foundation. The layering of the soil is indicated in colors with the layers of clay (brown), till (blue) and bedrock (gray). (For interpretation of the references to color in this figure legend, the reader is referred to the web version of this article.)

5. Experimental setup

The experimental investigations were performed using two measurement setups. The first setup considers the driven piles alone before casting of the concrete cap. The accelerations of all piles are measured when excitation is applied to each pile top. The measurements were performed five months after the piles had been driven, allowing excess pore pressures due to installation to even out. Measurements of only the pile top's responses were also conducted after two months. The second setup concerns the measurement of translational and rotational responses of the pile group. The tests were performed two months after the pile top measurements and one month after casting of the concrete cap.

5.1. Measurement equipment

The dynamic tests were performed with excitation from an impact hammer of model Dytran 5803A IEPE with a mass of 5.5 kg. Acceleration of the pile tops and the pile cap were measured by means of accelerometers of models PCB 393A01 and PCB 393B31. The response measurements within the piles were performed using a Geotomographie DDS presented in Fig. 4(a), equipped with two stations with PCB 66332APZ1 accelerometers mounted in a triaxial arrangement. The vertical spacing between the two stations is one meter. The equipment was originally designed for down-hole and cross-hole measurements where the coupling of the stations to the borehole is achieved by pneumatic clamping, allowing an arbitrary number of measurement points along each pile.

5.2. Setup 1: Pile tops

Fig. 5 presents an overview of the first setup where only the piles are present. Each pile was instrumented with six accelerometers at the top. Excitation was applied in the two horizontal directions at the same height and on the opposite side to where the sensors were mounted. Applying impacts at the top of the piles in the vertical direction inevitably produces a rotation of the pile cross-section as the piles cannot be excited at the center of the cross-section due to the presence of the

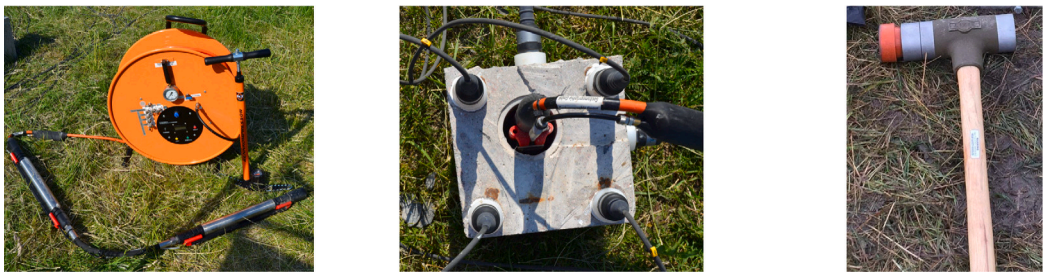

(a) (b) (c)

Fig. 4. Measurement equipment (a) Geotomographie DDS with pneumatic clamping of two triaxial measurement stations, (b) mounted in one of the piles together with PCB 393A01 accelerometers and (c) a Dytran 5803 A impact hammer.

Fig. 5. Measurement setup for the tests on the piles before the casting of the pile cap. The numbering of the piles P1 to P4 are indicated on the side of each pile.

pipe. Therefore, the vertical impacts were applied as close as possible to the center and the signals obtained from the four vertically orientated sensors were averaged, aimed at cancelling the influence of cross-sectional rotations. The setup further allows for obtaining the rotations of the pile cross-sections from the vertical acceleration measurements. In each test, a minimum of fifteen hammer impacts were applied in the vertical and two horizontal directions at each pile. Measurements at depth were performed by mounting the accelerometers within one of the piles at the desired depth and applying impacts in the three directions at the top of each one of the piles. This was repeated with the sensors mounted in each one of the piles for all the depths considered. For piles P1 and P4, two setups were performed at the depths (0.75 m, 1.75 m) and (2.75 m, 3.75 m) whereas for the longer piles P2 and P3 additional measurements at 4.75 m were performed, resulting in a total of ten setups.

5.3. Setup 2: Pile group

Fig. 6 presents the instrumentation for the test performed on the pile group. Seven accelerometers were installed on the pile cap with five mounted in the vertical direction ($a_1 - a_5$) and two in the horizontal directions (a_6 and a_7). The excitation was applied in the vertical direction by hammer impacts at position `Fz1` to characterise the response of the piles and the pile group due to a vertical load. Vertical impacts were additionally applied at positions `Fz2` and `Fz3` to obtain the rotational impedances of the pile cap around the horizontal x- and y-axis, respectively, assuming the pile cap to behave as a rigid block in the frequency range of interest. Horizontal excitations were applied along the two perpendicular horizontal axes, where the excitation and measurement points were positioned at the mid height of the concrete cap.

6. Results

From the impact tests, the frequency response functions are estimated from multiple impacts using the H_1 estimator, assuming the input signal to be free of any noise [49]. The estimated acceleration frequency response functions are integrated to receptances by division with $(\mathrm{i}\omega)^2$. The receptances at the pile tops and the pile cap are subsequently inverted in order to obtain the impedances. The complex valued impedance $Z_{ij}(\omega)$ represents the dynamic stiffness and damping of the foundation in the degree of freedom i related to the displacement or rotation in degree of freedom j where the real part $\mathrm{Re}(Z_{ij}(\omega))$ represents the frequency dependent stiffness and inertia, and the imaginary part $\mathrm{Im}(Z_{ij}(\omega))$ the damping.

6.1. Structural impedances of piles

Fig. 7 compares the experimentally and numerically obtained vertical and horizontal impedances at the top of the individual piles. While the experimentally determined impedances in the horizontal directions are very similar for all the piles in the group, the vertical impedances are different for the sets (`P1,P4`) and (`P2,P3`). This is due to the difference in length of the piles, where the shorter piles P1 and P4 have a higher stiffness than the longer ones. The horizontal impedances, on the other hand, are not affected by the difference in pile lengths. This is explained by the fact that the active length of a pile under lateral excitation is shorter than the total length of the piles, and is therefore almost unaffected by the depth of penetration into the non-cohesive soil [41]. The numerically predicted impedances are overestimated in both the vertical and horizontal direction. It should be noted that the numerical model assumes a pile that extends to a depth of 7.4 m, and therefore an even larger model error should be expected in the vertical impedance if considering the bedrock positioned at the actual pile lengths.

6.2. Pile–soil–pile interaction of free-top piles

The interaction between the piles in the group is illustrated by relating the motion of the excited pile to the motion of the receiving piles at the soil's surface by the pile interaction factor defined as:

$$\alpha_{ij}(\omega) = \frac{\text{displacement/rotation of pile } i \text{ due to a load at pile } j}{\text{displacement/rotation of pile } j \text{ due to a load at pile } j} \quad (1)$$

The real and imaginary parts of the interaction factor describe the amplitude and phase of the receiver pile relative to the displacement or rotation of the loaded pile, which govern the dynamic interaction effects in the pile group when joined together at the surface [4,15,16]. If the interaction factor is a purely positive or negative real number, the receiver pile moves in- or out of phase with the excited pile, respectively. This interaction between the piles gives rise to constructive or destructive interference with the forced motion of each pile when

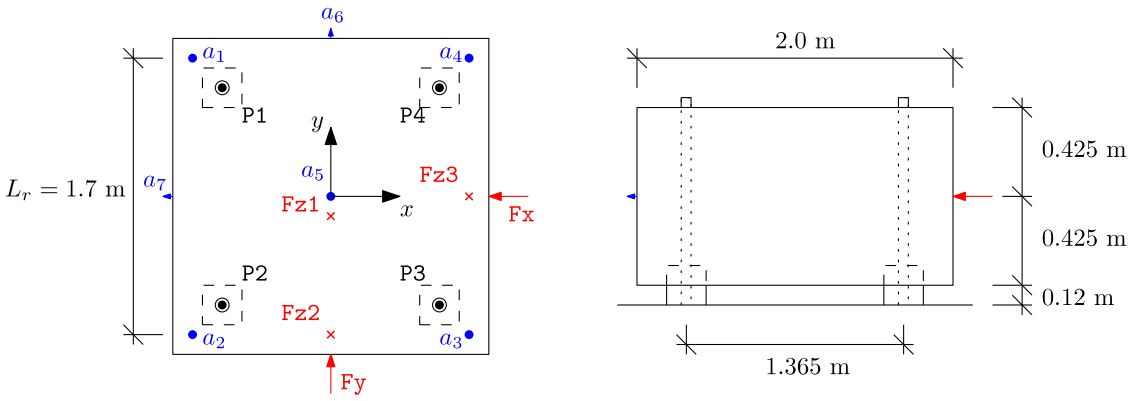

Fig. 6. Measurement setup and dimensions for the 2 × 2 pile group concrete cap with accelerometers indicated by a_j, piles by P1–4 and excitation points by F.

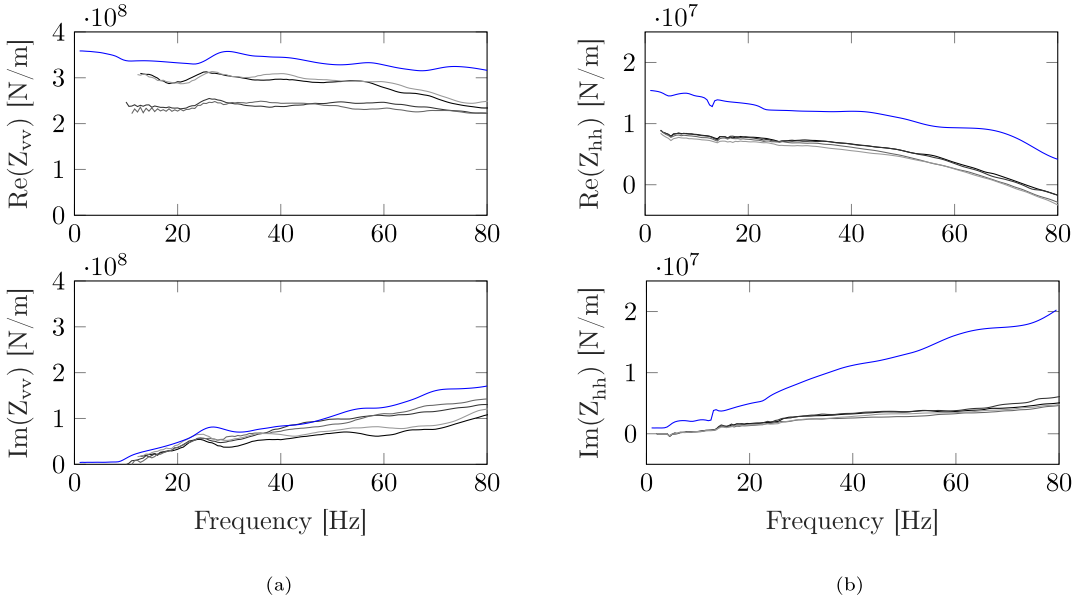

Fig. 7. Real (top) and imaginary part (bottom) of experimental pile top impedances for piles P1 to P4 (black to light gray) compared to the numerically predicted impedances (blue line) in the (a) vertical and (b) horizontal directions. (For interpretation of the references to color in this figure legend, the reader is referred to the web version of this article.)

the group of piles is loaded through e.g. a rigid pile cap, resulting in either a reduction or increase in the dynamic group stiffness.

Fig. 8 presents the interaction factors for horizontal translation due to a horizontal load ($\alpha_{hh,ij}$), cross sectional rotations due to a horizontal load ($\alpha_{h\theta,ij}$) and vertical translations due to a vertical load ($\alpha_{vv,ij}$). The horizontal interaction factors are presented only considering the load applied to the piles in the x-direction and rotations measured around the y-axis, with reference to Fig. 6. The experimentally obtained interaction factors are compared to the ones obtained from the numerical model. The horizontal interaction factors are influenced by the position of the receiver pile with respect to the direction of excitation, as it governs the type of waves induced in the soil by the motion of the excited pile [16]. Therefore, the piles are categorised based on the angle φ between the line of the two piles considered and the x-direction, which is the direction of horizontal excitation. In Figs. 8(b) and 8(c), it is observed that the piles that are subjected mainly to longitudinal waves, i.e. for which $\varphi = 0°$, move out of phase at about 45 Hz. The piles for which $\varphi = 90°$ are mainly subjected to horizontally polarized S-waves that have a lower wave speed, and move out of phase with the loaded pile at about 30 Hz. The diagonal pile pairs are subjected to a combination of these two wave types and also move out of phase for a frequency of about 30 Hz. Naturally, as the vertical load case is symmetric with respect to the considered values of φ, it should have no significant influence on the vertical interaction factors, which is verified in Figs. 8(b) and 8(c).

The interaction factors obtained from the numerical model agrees fairly well with the experimental results. The amplitudes of α_{hh} and $\alpha_{h\theta}$ for the pile pairs where $\varphi = 90°$ are overestimated, but the relation between the real and imaginary part, i.e. the phase, is well captured up to about 55 Hz. The interaction factor α_{hh} for the diagonal piles is on the other hand quite well represented in amplitude, but slightly shifted towards lower frequencies in the oscillations of the real and imaginary parts. In all the horizontal and cross horizontal-rotational interaction factors, the first three natural frequencies of the soil deposit can be observed as local peaks at 5, 14 and 26 Hz, which can also be observed as dents in the pile impedances of Fig. 7(b).

The predicted vertical interaction factors α_{vv} are similar in character to the measured ones. However, a shift in frequency from 27 to 30 Hz of the out of phase motion is observed when comparing the measurements to the numerical predictions. For floating piles in a homogeneous soil, this out of phase motion occurs at the frequency where the pile spacing is equal to half the wavelength of horizontally propagating vertically polarized S-waves [15]. This indicates that the effective S-wave speed in the soil between the piles is slightly higher in the model. Measurements performed at depth due to the loads applied at the surface allows to study the global motion of the group of piles in the

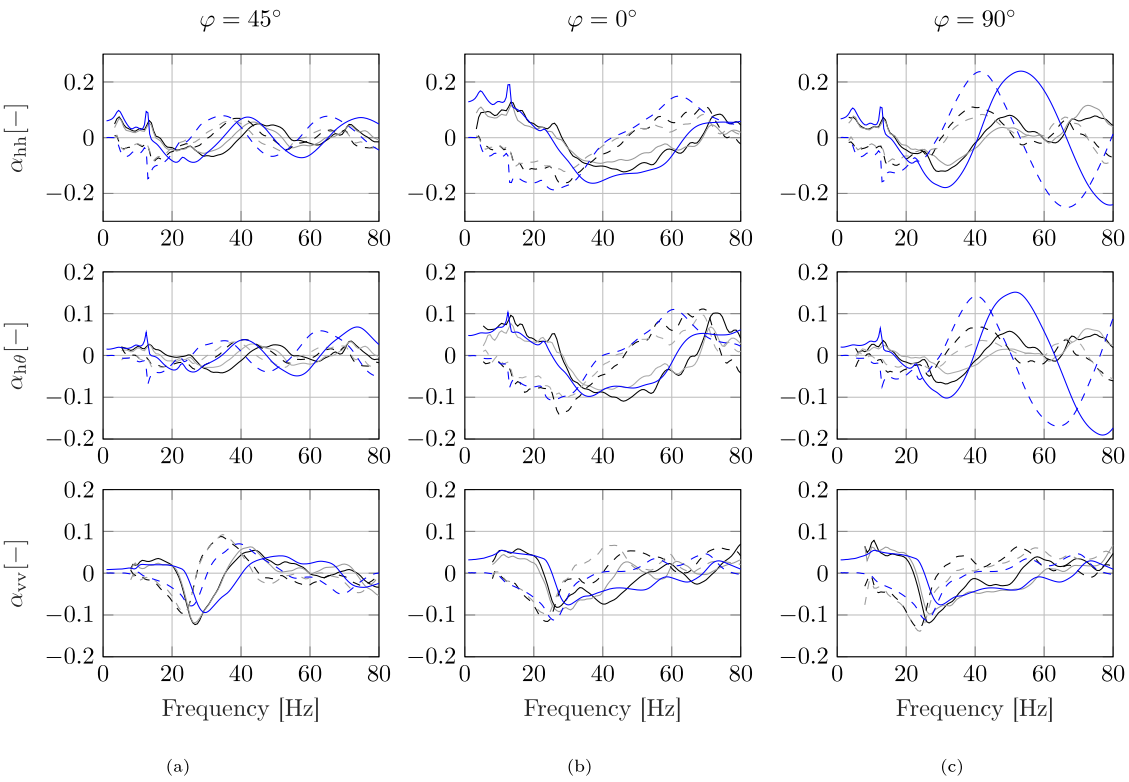

Fig. 8. Real (solid lines) and imaginary parts (dashed lines) of pile interaction factors (black and gray) (a) α_{13} and α_{42}, (b) α_{14} and α_{32} and (c) α_{12} and α_{43} of horizontal displacement due to a horizontal load (top), cross section rotation due to a horizontal load (middle) and vertical displacement due to a vertical load (bottom) obtained from the measurements compared to the numerical predictions (blue). (For interpretation of the references to color in this figure legend, the reader is referred to the web version of this article.)

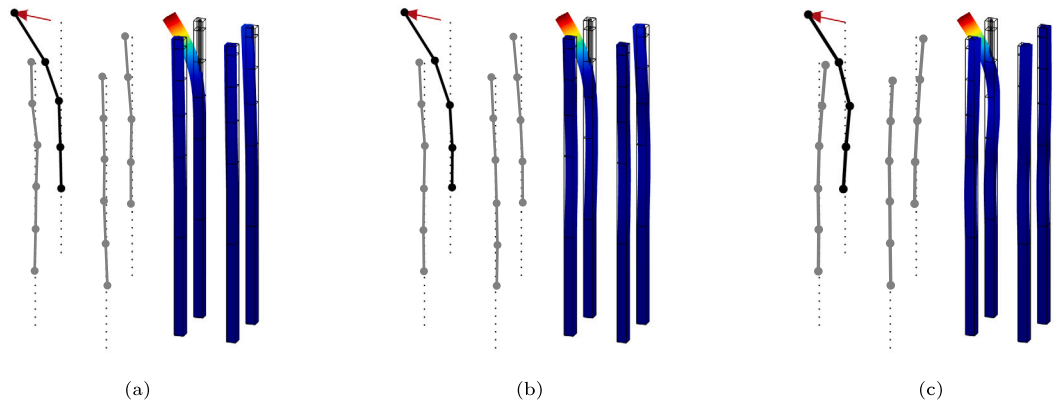

Fig. 9. Measured (left) and predicted (right) deflections of free-top piles due to horizontal pile head excitation at pile P1 at frequencies (a) 5, (b) 14 and (c) 26 Hz in the horizontal direction. The displacements are identically scaled for the measured and computed illustrations.

soil. Fig. 9 presents a comparison between snapshots of the measured and computed harmonic motion of the group of free-top piles due to a force applied in the horizontal direction at the top of pile P1. The wavelengths associated with standing waves in the clay can be observed not only for the excited pile, but also for the three receiving piles.

The deformations are largely concentrated in the upper portion of the soil, agreeing with the numerical predictions, further supporting the observation that the horizontal impedances of the piles are practically unaffected by the total length of the piles due to the active length being smaller than the total depth of the stratum.

6.3. Temporal variations due to environmental conditions

The sensitivity of the horizontal impedance of the single pile to the properties of the soil closest to the surface and the ability of the model to capture the interaction between the piles due to horizontal excitation, as presented in Fig. 8, suggest that the discrepancies between the measured and predicted horizontal pile impedances are due to local effects at the excited pile. This is consistent with findings by other authors [31,41,50]. Consideration of a free length closest to the soil's surface between the pile and the soil, or a weakened zone at the pile–soil interface have been suggested to obtain more accurate predictions of the horizontal impedance of single piles [51]. However,

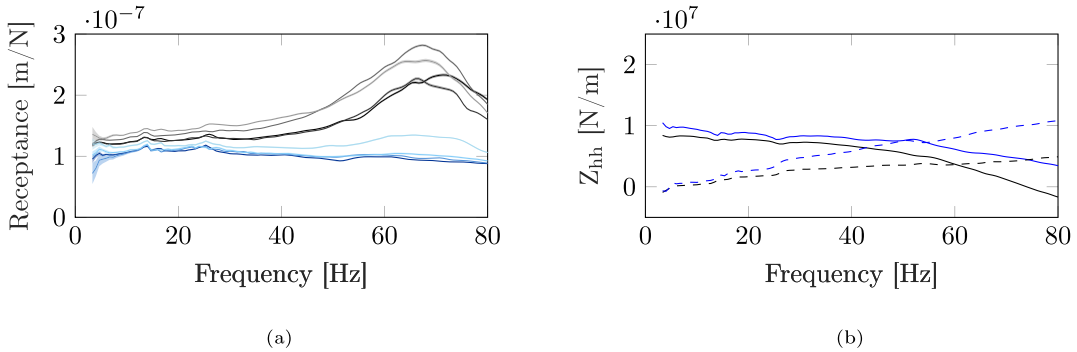

Fig. 10. Comparison between measurement results in spring (blue) and summer (black) of horizontal pile (a) receptances with 95% confidence bounds for piles P1 to P4 (dark to light) and (b) real (solid lines) and imaginary part (dashed lines) impedance of pile P1. (For interpretation of the references to color in this figure legend, the reader is referred to the web version of this article.)

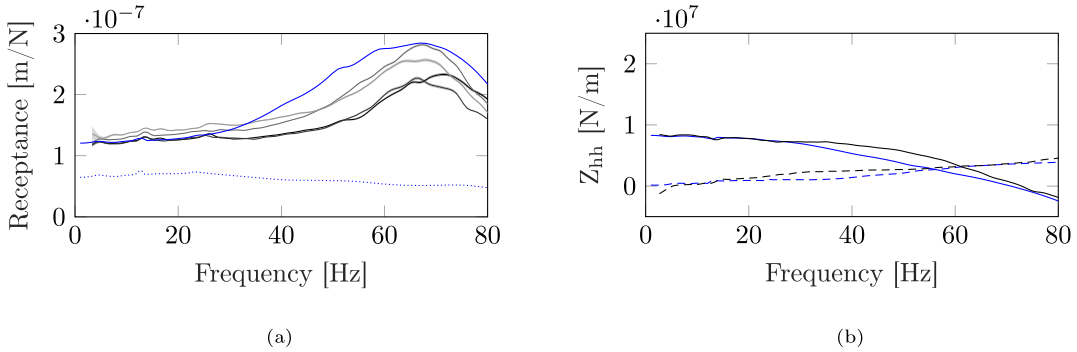

Fig. 11. Numerical results (blue) based on a model of a single pile assuming a loss of contact with the most shallow soil layer extending to a depth of 0.6 m compared to the (a) horizontal receptances obtained from the original model (blue dotted line) and the measurements for piles P1 to P4 in the summer (black to light gray) with 95% confidence bounds and (b) the measured real (black solid lines) and imaginary (black dashed lines) parts of the impedance of pile P1. (For interpretation of the references to color in this figure legend, the reader is referred to the web version of this article.)

an appropriate selection of parameters is required for these model adjustments to obtain accurate results. Moreover, these considerations might not be appropriate for pile groups, which are not as sensitive as single piles to the conditions closest to the surface [52].

At the present site, and under similar soil conditions, the mechanical properties of the layer of soil closest to the surface change over time due to the environmental conditions [44]. Therefore, the change in environmental conditions are expected to influence the horizontal impedances of the piles. Fig. 10(a) compares the horizontal receptances of the four piles measured in summer and in the spring three months before. In both cases, the impacts applied to the piles were of approximately the same magnitude. A pronounced peak is observed around 70 Hz for all the piles during the measurements performed in summer. This peak can only be distinguished for pile P4 in the spring, but with a significantly lower amplitude. The real and imaginary parts of the impedances for pile P1 in spring and in summer are compared in Fig. 10(b). The impedance of the pile is higher over the entire frequency range considered when measured in spring, but especially in the upper part of the band associated with the observed resonance. However, the impedance is still significantly lower compared to the predicted one of Fig. 7(b). This indicates that while environmental conditions might influence the horizontal impedance of the piles, the soil closest to the surface is not accurately enough described by the layered soil model to capture the true horizontal impedance of the individual piles.

In summer, it was observed that drying of the crust had occurred, causing it to crack up at the surface such that stakes set out at the site had become loose. It was therefore investigated whether a loss of contact between the piles and the soil could explain the observed resonance phenomenon. Fig. 11 compares the pile top response of all four piles and the impedance of pile P1 to the numerical results obtained from a model of a single pile with the soil modified by reducing the depth of the uppermost soil layer to 0.6 m and separating this layer from the pile with a spacing of 25 mm. The loss of contact between the pile and the soil dramatically decreases the horizontal stiffness of the pile, making it more flexible and giving rise to a resonance phenomenon in the pile similar to what was observed in the measurements. The correspondence between the simulations and the measurements indicate that the inconsistencies observed in Fig. 10 are indeed caused by a change in the contact conditions between the piles and the soil closest to the surface. This shows not only the difficulty in predicting the horizontal impedance of piles, but also that slight variations in the condition of the topmost soil between april and june can significantly influence the impedance that is measured.

6.4. Response of pile group joined at the surface

Fig. 12 presents a comparison between experimentally and numerically obtained receptances in the vertical and horizontal directions of the concrete pile cap and the responses at depth within the diagonally placed piles P1 and P3. The vertical frequency response is obtained as the average of the recorded signals from accelerometers $a_1 - a_5$ due to the impact test at the position Fz1. The horizontal responses are close to identical for the two perpendicular directions and only the response due to the impact load Fx is presented here.

As for the free-top piles, the resonance frequencies in horizontal motion are identified as peaks in the response spectra. The third natural frequency is not well pronounced in the receptance plots, but is more easily located in the accelerance spectrum not shown here. The responses at depth show slightly different amplitudes in the two diagonally placed piles in the upper 2 m, while the same responses are measured at deeper levels. The model captures the horizontal motion of the foundation well apart from a slight shift in the predicted resonance

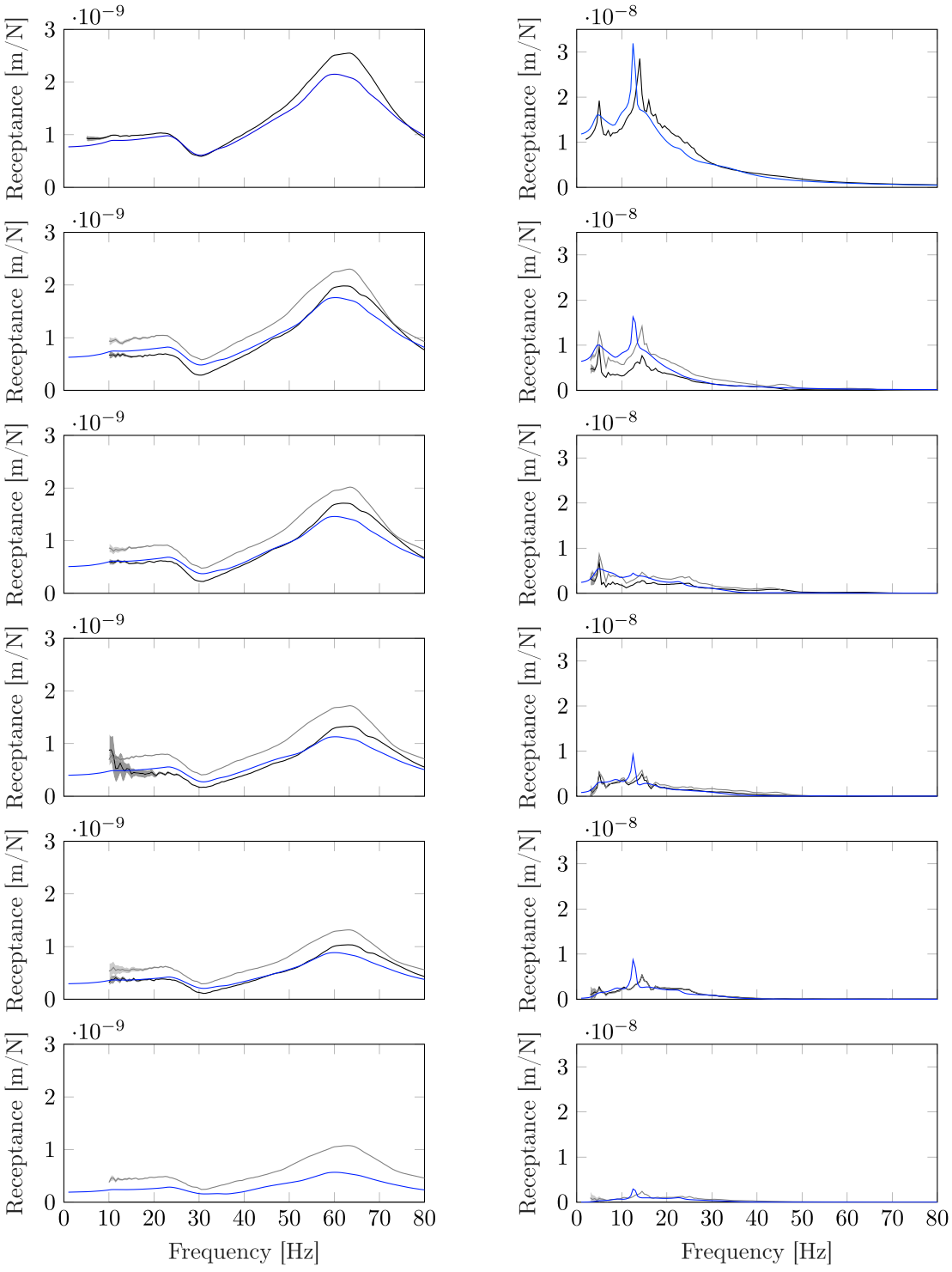

Fig. 12. Receptances in the vertical direction due to the vertical load Fz1 (left) and horizontal direction due to the horizontal load Fx (right). Results are presented for the pile cap (top row) and at the depths 0.75, 1.75, 2.75, 3.75 and 4.75 m within the piles P1 (black line) and P3 (gray line) compared to numerical predictions (blue line). The 95% confidence bounds on measured quantities are indicated by a shaded region. (For interpretation of the references to color in this figure legend, the reader is referred to the web version of this article.)

frequencies. The vertical response shows a modest peak at 23 Hz, a trough at 30 Hz and a more pronounced peak at 63 Hz. As the foundation is not fully symmetric and a small eccentricity is present for the applied impact load, the piles show slightly different amplitudes in the measured responses. The numerical predictions capture the vertical responses, but the amplitude of the response around peak in at 63 Hz is slightly underestimated. The presence of this peak is the result of inertial interaction between the piles and the mass of the pile cap. That is, considering the foundation as massless eliminates this part of the response altogether. Due to a low signal-to-noise ratio at frequencies below 10 Hz, the measurements at depth in the vertical direction show a low coherence in this frequency range and are therefore considered inaccurate.

Fig. 13 presents the measured and computed snapshots of harmonic displacements of the pile foundation at its horizontal resonance frequencies when subjected to horizontal excitation. The wavelengths

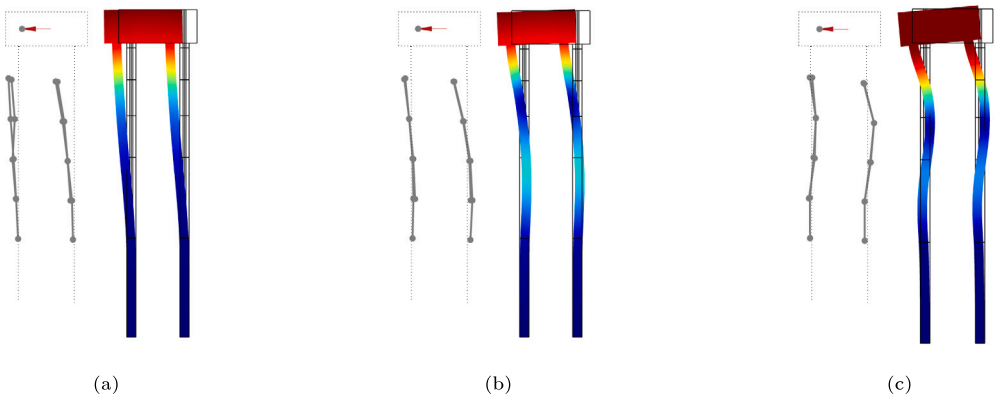

Fig. 13. Measured (left) and computed (right) harmonic displacements at the (a) first (b) second and (c) third resonance frequency of the pile group due to horizontal excitation. The displacements are identically scaled for the measured and computed illustrations.

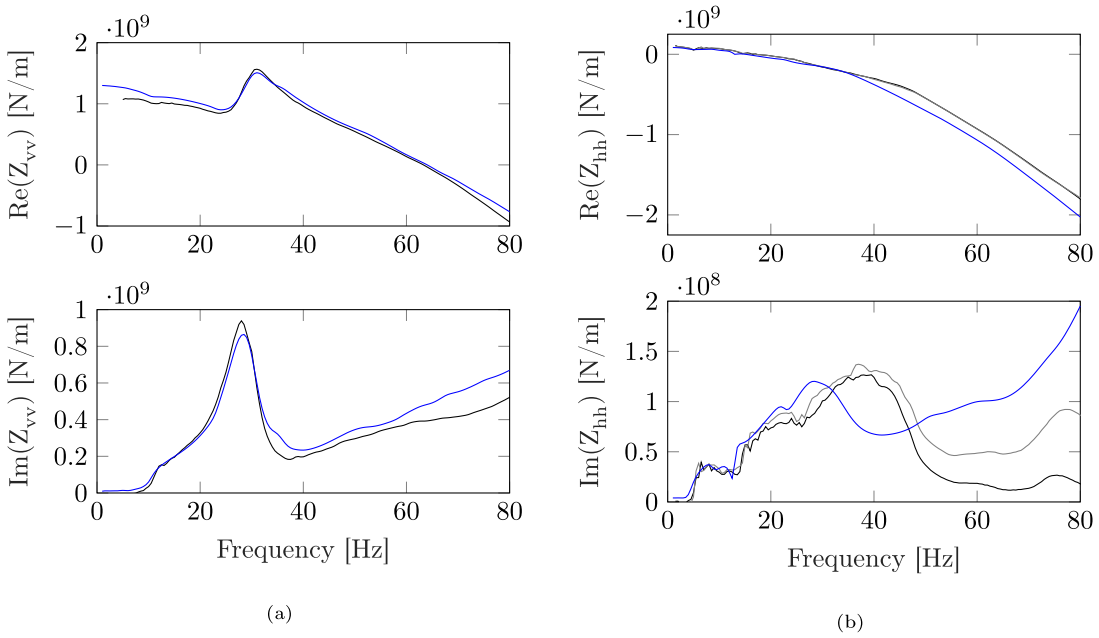

Fig. 14. Real (top) and imaginary part (bottom) of the experimental (black and gray lines) and numerical (blue line) pile group impedance in the (a) vertical and (b) two horizontal directions. (For interpretation of the references to color in this figure legend, the reader is referred to the web version of this article.)

associated with the standing waves in the clay are clearly seen for the three frequencies considered and correspond well with the numerical results.

6.5. Structural impedances of the joined pile group

Fig. 14 presents the measured and predicted structural impedances of the joined pile group in the vertical and horizontal directions. The vertical impedances are obtained from the impact test `Fz1` and the average vertical response of sensors $a_1 - a_5$. The horizontal impedances are obtained in both horizontal directions from the impact tests `Fx` and `Fy`. The impedances of the joined pile group are well predicted in both the vertical and horizontal directions. The peaks observed in the real and imaginary parts of the vertical impedance, caused by pile–soil–pile interaction, are well captured by the model. The measured vertical interaction factors of the piles in Fig. 8 indicate a frequency of 27 Hz where the piles move out of phase, whereas the numerical interaction factors are slightly shifted towards 30 Hz. The dominating interaction frequency highly depends upon the soil properties and the inter-spacing between the piles in the group. A change in soil properties, especially closest to the surface, can therefore have a significant influence on the apparent interaction frequency, which has been demonstrated in the literature using numerical models [14,53]. Consequently, the slight shift in frequency observed between the two measurements indicates that the stiffness of the soil, and therefore the effective wave speed between the piles, have slightly changed after construction of the pile cap. It should be noted that the inertia of the pile cap contributes to the real parts of the vertical and horizontal impedances as the term $-\omega^2 \mathrm{m}$, with m the mass of the pile cap. In the vertical direction, this makes the real part of the impedance become zero at 63 Hz, resulting in the resonance peak observed in Fig. 12. The imaginary part of the vertical impedance is slightly overestimated by the model for frequencies over 40 Hz, resulting in under-predicted response amplitudes near the resonance frequency where the response is mostly damping controlled.

The horizontal impedance of the pile group is well captured by the model up to a frequency of 30 Hz and the cut-off frequencies corresponding to the resonance frequencies of the clay are seen in the imaginary part of the horizontal impedance as the onset at 5 Hz and the local minima at 14 and 26 Hz. It is noted that despite the larger differences observed between measured and predicted horizontal impedances of the single piles, the prediction of the horizontal pile group impedance agree reasonably well with the measurements. These

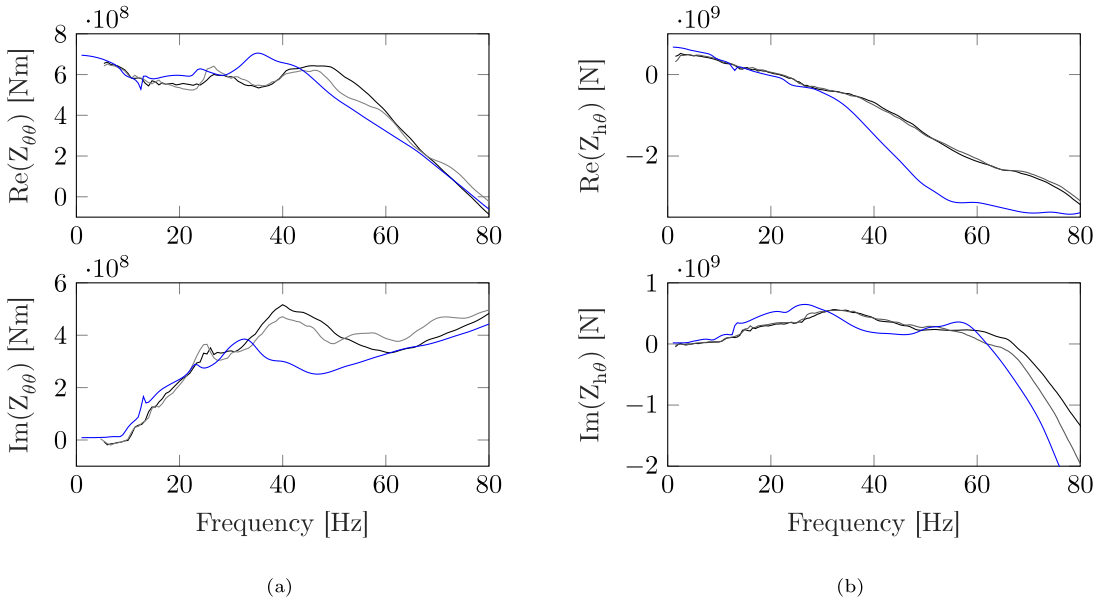

Fig. 15. Real (top) and imaginary part (bottom) of the experimental (black and gray lines) and numerical (blue line) pile group (a) rotational and (b) cross horizontal-rotational impedances. (For interpretation of the references to color in this figure legend, the reader is referred to the web version of this article.)

observations support numerical and previous experimental findings that pile groups are less influenced by the soil conditions closest to the surface than solitary piles [31,52].

The rotational and cross horizontal-rotational impedances are estimated from the impacts tests at positions Fz2 and Fz3. For Fz2 the impedances are calculated with reference to Fig. 6 as:

$$Z_{\theta\theta}(\omega) = -\frac{\omega^2 F_{z2}(\omega) L_r^2}{(a_1 + a_4) - (a_2 + a_3)} \tag{2}$$

$$Z_{\mathrm{h}\theta}(\omega) = -\frac{\omega^2 F_{z2}(\omega) L_r}{2a_6(\omega)} \tag{3}$$

Fig. 15 presents a comparison between the measured and predicted rotational and cross horizontal-rotational impedances. Experimental results obtained from the measurements of the rotations around the two horizontal axes are included, which illustrates that the rotational stiffness is almost unaffected by the differences in the length of the piles. The rotational impedance is well predicted by the model, apart from differences in the locations of the peaks in the spectra similar to what is found for the horizontal impedance.

Both horizontal and rotational numerical impedances, which are coupled, start to deviate from the measured ones for frequencies above 30 Hz. While the pile–soil–pile interaction is well captured by the model for the individual piles for both horizontal and cross horizontal-rotational motion, the increase in the pile group impedances due to pile–soil–pile interaction is found at a higher frequency of approximately 45 Hz, corresponding to the peaks in the real and imaginary parts of the impedances. As for the vertical impedance, this further indicates a lengthening of the wavelengths involved in the pile–soil–pile interaction, i.e. a stiffening of the soil. On the other hand, it is noted that the lateral natural frequencies of the clay are essentially the same in the measurements of the free piles and the pile cap. This indicates that the average soil properties are not significantly affected over the whole body of clay, and the variation in small-strain properties is probably localised in the upper part of the soil profile.

7. Conclusion

This paper presents the experimental results of the dynamic response of impact driven concrete piles and a 2 × 2 pile group for the purpose of model validation. The piles were driven at a test site where extensive site investigations have been performed and the small-strain properties required for modelling the soil have been determined by geophysical in situ methods, analysis of laboratory samples and empirical relations. The soil conditions consist of a 4.9 m layer of soft clay on top of a 2.5 m layer of till resting on a stiff bedrock.

Frequency response functions were measured in two stages of construction. First when the piles had been driven and were free at the surface and then after the concrete cap had been cast, joining the piles together at the surface. Excitation was applied to the pile tops and the pile cap by means of an instrumented impact hammer and the acceleration response of the piles and the pile cap were measured. Each pile was prepared in the factory with a central cylindrical cavity, allowing to install sensors in the field and to measure the response within the piles at depth using equipment for down-hole geophysical surveys. The measurements of the free top piles are used to obtain the individual pile impedances and pile-to-pile interaction factors, describing the interaction between the piles through the soil. The measurements of the vertical, horizontal, rotational and horizontal-rotational impedances of the pile group joined by the concrete cap are also presented.

A linear elastic three dimensional finite element model with perfectly matched layers is used to predict the dynamic characteristics of both the free individual piles and the joined pile group foundation, subjected to the same load cases as in the measurements. A design condition is considered for predicting the impedances of the foundation, meaning that the numerical predictions are obtained from a model based solely on the performed soil investigations and no attempt to update the model to better fit the measurement results have been performed. The numerical predictions are compared to the measurements to assess the ability of the model to capture the dynamic interaction between the soil and the foundation. The following conclusions from the study are made:

- The impedances of the pile group foundation on driven end-bearing concrete piles in soft clay are well predicted using a linear elastic three dimensional finite element model. In particular, the predicted variation of the vertical impedance with frequency due to pile–soil–pile interaction is in excellent agreement with the measurements.
- The vertical and horizontal impedances of the free top piles are not as well predicted as the group impedance.

- Horizontal impedances of the free top piles are found to be different between spring and summer. This is caused by a loss of contact between the pile and the topmost soil, showing that even small changes in the environmental conditions can significantly influence the measured pile impedance.
- Measured dynamic pile–soil–pile interaction factors clearly show the out-of-phase motion associated with an increase in foundation impedance within the studied frequency range. The corresponding interaction effects are also found in the measurements of the group impedances, validating previous theoretical findings.
- The horizontal impedances of the piles and the pile group are influenced by the clay layer's first three natural frequencies and are unaffected by the depth of the stiffer non-cohesive soil into which they are driven. The associated modes of the piles obtained from the model are in agreement with the measurements.

CRediT authorship contribution statement

Freddie Theland: Conceptualization, Methodology, Software, Writing– original draft, Investigation, Data curation, Formal analysis. **Geert Lombaert:** Supervision, Conceptualization, Methodology, Writing – review & editing. **Stijn François:** Conceptualization, Methodology, Writing – review & editing. **Costin Pacoste:** Conceptualization. **Fanny Deckner:** Supervision, Conceptualization, Methodology, Writing – review & editing. **Peter Blom:** Conceptualization. **Jean-Marc Battini:** Supervision, Conceptualization, Methodology, Writing – review & editing, Funding acquisition.

Declaration of competing interest

The authors declare that they have no known competing financial interests or personal relationships that could have appeared to influence the work reported in this paper.

Acknowledgments

This work is supported by the Development Fund of the Swedish Construction Industry (SBUF). The funding for experiments and site investigations is received from Vinnova, Trafikverket and the Richertska foundation. The financial support is gratefully acknowledged. The authors would also like to extend their gratitude towards Ragnvald Andersson for granting unlimited access to the test site used for the experiments performed in this work.

References

[1] Axelsson G. Design of piles - Swedish practice. In: ISSMGE - ETC 3 international symposium on design of piles in Europe, Leuven, Belgium. 2016.
[2] Commission on Pile Research. Pile statistics for Sweden 2019. 2020, URL: http://www.palkommissionen.org/web/page.aspx?refid=73.
[3] Kausel E. Advanced structural dynamics. Cambridge University Press; 2017, http://dx.doi.org/10.1017/9781316761403.
[4] Dobry R, Gazetas G. Simple method for dynamic stiffness and damping of floating pile groups. Géotechnique 1988;38(4):557–74.
[5] Makris N, Badoni D. Seismic response of pile groups under oblique-shear and Rayleigh waves. Earthq Eng Struct Dyn 1995;24(4):517–32.
[6] Gazetas G, Fan K, Kaynia A, Kausel E. Dynamic interaction factors for floating pile groups. J Geotech Eng 1991;117(10):1531–48.
[7] Saitoh M, Padrón LA, Aznárez JJ, Maeso O, Goit CS. Expanded superposition method for impedance functions of inclined-pile groups. Int J Numer Anal Methods Geomech 2016;40(2):185–206.
[8] Dai W, Shi C, Tan Y, Rojas F. A numerical solution and evaluation of dynamic stiffness of pile groups and comparison to experimental results. Eng Struct 2017;151:253–60.
[9] Taherzadeh R, Clouteau D, Cottereau R. Simple formulas for the dynamic stiffness of pile groups. Earthq Eng Struct Dyn 2009;38(15):1665–85.
[10] Dezi F, Carbonari S, Leoni G. A model for the 3D kinematic interaction analysis of pile groups in layered soils. Earthq Eng Struct Dyn 2009;38(11):1281–305.
[11] Carbonari S, Morici M, Dezi F, Leoni G. Analytical evaluation of impedances and kinematic response of inclined piles. Eng Struct 2016;117:384–96.
[12] Kaynia AM, Kausel E. Dynamics of piles and pile groups in layered soil media. Soil Dyn Earthq Eng 1991;10(8):386–401.
[13] Padrón L, Aznárez J, Maeso O, Saitoh M. Impedance functions of end-bearing inclined piles. Soil Dyn Earthq Eng 2012;38:97–108.
[14] Álamo GM, Martínez-Castro AE, Padrón LA, Aznárez JJ, Gallego R, Maeso O. Efficient numerical model for the computation of impedance functions of inclined pile groups in layered soils. Eng Struct 2016;126:379–90.
[15] Gazetas G, Makris N. Dynamic pile-soil-pile interaction. Part I: Analysis of axial vibration. Earthq Eng Struct Dyn 1991;20(2):115–32.
[16] Makris N, Gazetas G. Dynamic pile-soil-pile interaction. Part II: Lateral and seismic response. Earthq Eng Struct Dyn 1992;21(2):145–62.
[17] Masoumi HR, Degrande G, Holeyman A. Pile response and free field vibrations due to low strain dynamic loading. Soil Dyn Earthq Eng 2009;29(5):834–44.
[18] Elkasabgy M, El Naggar MH. Dynamic response of vertically loaded helical and driven steel piles. Can Geotech J 2013;50(5):521–35.
[19] Tantayopin K, Thammarak P. Effect of soft soil layer on local dynamic response of floating pile under harmonic lateral loading. Can Geotech J 2017;54(12):1637–46.
[20] Esmaeilzadeh Seylabi E, Kurtuluş A, Stokoe KH, Taciroglu E. Interaction of a pile with layered-soil under vertical excitations: field experiments versus numerical simulations. Bull Earthq Eng 2017;15(9):3529–53.
[21] Capatti MC, Dezi F, Carbonari S, Gara F. Full-scale experimental assessment of the dynamic horizontal behavior of micropiles in alluvial silty soils. Soil Dyn Earthq Eng 2018;113:58–74.
[22] Han Y, Vaziri H. Dynamic response of pile groups under lateral loading. Soil Dyn Earthq Eng 1992;11(2):87–99.
[23] Blaney GW, O'Neill MW. Dynamic lateral response of a pile group in clay. Geotech Test J 1989;12(1):22–9.
[24] Burr JP, Pender MJ, Larkin TJ. Dynamic response of laterally excited pile groups. J Geotech Geoenviron Eng 1997;123(1):1–8.
[25] Biswas S, Manna B. Experimental and theoretical studies on the nonlinear characteristics of soil-pile systems under coupled vibrations. J Geotech Geoenviron Eng 2018;144(3):04018007.
[26] Choudhary SS, Biswas S, Manna B. Effect of pile arrangements on the dynamic coupled response of pile groups. Geotech Geol Eng 2021;39:1573–978.
[27] Cao X, Wang S, Gong W, Wu W, Dai G, Zhou F. Experimental and theoretical study on dynamic stiffness of floating single pile and pile groups in multi-layered soil. Soil Dyn Earthq Eng 2022;157:107282.
[28] El Sharnouby BB, Novak M. Dynamic experiments with group of piles. 1984;110(6):719–737.
[29] Goit CS, Saitoh M. Model tests on horizontal impedance functions of fixed-head inclined pile groups under soil nonlinearity. J Geotech Geoenviron Eng 2014;140(6):04014023.
[30] Kobori T, Miura K, Nakazawa M, Hijikata K, Miyamoto Y, Moroi T, Kobayashi Y. Study on dynamic characteristics of a pile group foundation. 1991;(45).
[31] El-marsafawi H, Han YC, Novak M. Dynamic experiments on two pile groups. J Geotech Eng 1992;118(4):576–92.
[32] Manna B, Baidya DK. Nonlinear dynamic response of piles under horizontal excitation. J Geotech Geoenviron Eng 2010;136(12):1600–9.
[33] Novak M, Grigg FR. Dynamic experiments with small pile foundations. Can Geotech J 1976;13(4):372–85.
[34] Manna B, Baidya DK. Dynamic nonlinear response of pile foundations under vertical vibration-theory versus experiment. Soil Dyn Earthq Eng 2010;30(6):456–69.
[35] Capatti MC, Dezi F, Carbonari S, Gara F. Dynamic performance of a full-scale micropile group: Relevance of nonlinear behaviour of the soil adjacent to micropiles. Soil Dyn Earthq Eng 2020;128:105858.
[36] Goit CS, Saitoh M, Mylonakis G, Kawakami H, Oikawa H. Model tests on horizontal pile-to-pile interaction incorporating local non-linearity and resonance effects. Soil Dyn Earthq Eng 2013;48:175–92.
[37] Goit CS, Saitoh M. Experimental approach on the pile-to-pile interaction factors and impedance functions of inclined piles. Géotechnique 2016;66(11):888–901.
[38] Ullah MS, Yamamoto H, Goit CS, Saitoh M. On the verification of superposition method of kinematic interaction and inertial interaction in dynamic response analysis of soil-pile-structure systems. Soil Dyn Earthq Eng 2018;113:522–33.
[39] Zafar U, Goit C, Saitoh M. Experimental and numerical investigations on vertical dynamic pile-to-pile interactions considering soil and interface nonlinearities. Bull Earthq Eng 2021.
[40] Dezi F, Gara F, Roia D. Linear and nonlinear dynamic response of piles in soft marine clay. J Geotech Geoenviron Eng 2017;143(1):04016085.
[41] Gazetas G. Seismic response of end-bearing single piles. Int J Soil Dyn Earthq Eng 1984;3(2):82–93.
[42] Lambe TW. Predictions in soil engineering. Géotechnique 1973;23(2):151–202.

[43] Google Earth Pro V7337786. Brottby, Sweden. 59°35'24.3"N 18°10'26.0"W, Eye alt 383 m. Maxar technologies 2020. 2020, http://www.earth.google.com [September 21, 2020].
[44] Theland F, Lombaert G, François S, Pacoste C, Deckner F, Battini J-M. Assessment of small-strain characteristics for vibration predictions in a Swedish clay deposit. Soil Dyn Earthq Eng 2021;150:106804.
[45] Nogami T. Dynamic group effect in axial responses of grouped piles. J Geotech Eng 1983;109(2):228–43.
[46] Mechanical vibration and shock – Evaluation of human exposure to whole-body vibration – Part 2: Vibration in buildings (1 Hz to 80 Hz). ISO 2631-2:2003, 2003, Geneva, CH: International Organization for Standardization; 2003.
[47] Emani P, Maheshwari B. Dynamic impedances of pile groups with embedded caps in homogeneous elastic soils using CIFECM. Soil Dyn Earthq Eng 2009;29(6):963–73.
[48] Basu U, Chopra AK. Perfectly matched layers for time-harmonic elastodynamics of unbounded domains: theory and finite-element implementation. Comput Methods Appl Mech Engrg 2003;192(11):1337–75.
[49] Bendat J. Statistical errors in measurement of coherence functions and input/output quantities. J Sound Vib 1978;59(3):405–21.
[50] Wang MC, Liao WP. Active length of laterally loaded piles. J Geotech Eng 1987;113(9):1044–8.
[51] Novak M. Piles under dynamic loads. In: Second international conference on recent advances in geotechnical earthquake engineering and soil dynamics. (12). 1991.
[52] Kaynia AM. Dynamic stiffness and seismic response of pile groups (Ph.D. thesis), Massachusetts institute of technology; 1982.
[53] Kaynia AM, editor. Analysis of pile foundations subject to static and dynamic loading. 1st ed.. CRC Press; 2021, http://dx.doi.org/10.1201/9780429354281.